Photolabile Derivatives of ^{125}I-Apamin: Defining the Structural Criteria Required for Labeling High and Low Molecular Mass Polypeptides Associated with Small Conductance Ca^{2+}-Activated K^+ Channels†

Jonathan D. F. Wadsworth,*,‡ Kevina B. Doorty,‡ C. Robin Ganellin,§ and Peter N. Strong‡

Neuromuscular Unit, Department of Paediatrics and Neonatal Medicine, Royal Postgraduate Medical School, Hammersmith Hospital, London W12 0NN, U.K., and Christopher Ingold Laboratories, Department of Chemistry, University College London, London WC1H 0AJ, U.K.

Received January 31, 1996; Revised Manuscript Received April 1, 1996⊗

ABSTRACT: The structure of apamin-sensitive Ca^{2+}- activated K^+ channels has been investigated using high-affinity, photolabile azidoaryl derivatives of ^{125}I-[α-formyl-Cys_1]apamin and ^{125}I-[ϵ-formyl-Lys_4]-apamin. Labeling patterns suggest that similar structural constraints are required for labeling analogous polypeptides associated with distinct channel subtypes. When photoprobes are coupled at the ϵ-amino-Lys_4 position of apamin, comparable low molecular mass (∼30 kDa) polypeptides are efficiently labeled on either brain or liver plasma membranes, irrespective of the structure of the photoprobe. However, when photoprobes are coupled at the α-amino-Cys_1 position of apamin, the pattern of labeling on both brain and liver plasma membranes varies, depending upon the length of the spacer arm incorporated into the photoprobe. Spacer arms of approximately 8−9 Å efficiently label only high molecular mass polypeptides (86, 59 kDa), accompanied by weak, variable labeling of a 44-kDa component. A shorter spacer arm (5.7 Å) results in feeble labeling of 86- and 59-kDa polypeptides and barely detectable labeling of 44- and ∼30-kDa polypeptides. In contrast, a long spacer arm (12.8 Å) efficiently labels only ∼30-kDa polypeptides. These findings point to close similarities in the topography of the ^{125}I-apamin binding site present on pharmacologically distinct subtypes of apamin-sensitive Ca^{2+}- activated K^+ channels and indicates that heterooligomeric association of high and low molecular mass polypeptide subunits may be a general structural feature of members belonging to this family of K^+ channels.

Apamin, an 18-amino-acid peptide neurotoxin ($M_r \sim 2000$) from the venom of the European honeybee *Apis mellifera*, potently and selectively inhibits small conductance (<20 pS) Ca^{2+}-activated K^+ channels (SK_{Ca} channels)[1] in both the central nervous system and peripheral tissues [reviewed by Brewster and Strong (1992)]. The fact that ^{125}I-apamin recognizes single classes of noninteracting binding sites on plasma membranes prepared from various tissues which express functional SK_{Ca} channels (Hugues *et al*., 1982a; Marqueze *et al*., 1987; Wadsworth *et al*., 1994), strongly implicates apamin binding proteins as structural components of the SK_{Ca} channel. To-date, cross-linking experiments using ^{125}I-apamin and photoreactive derivatives of the toxin have provided the only insights into putative SK_{Ca} channel structure.

Following the original demonstration by Lazdunski's group that a ∼30-kDa polypeptide is closely associated with the apamin binding site on neuronal membranes (Hugues *et al*., 1982b), the elegant work of Seagar, Couraud, and colleagues (Seagar *et al*., 1985, 1986) led to the realization that this polypeptide might be part of a larger heterooligomeric complex. By systematically derivatizing ^{125}I-apamin on one or the other of its two free amino groups (α-Cys_1 or ϵ-Lys_4) with a photolabile aryl azide, Seagar *et al*. were able to exclusively label two distinct groups of polypeptides (86, 59 kDa and 33, 22 kDa). Further studies from Lazdunski and colleagues (Auguste *et al*., 1989) demonstrated that labeling patterns varied, dependent on the chemical structure of the photoprobe. In particular, whereas all photolabile species labeled a ∼30-kDa polypeptide, the photoprobe used by Seagar *et al*. was the only probe tested that could label the 86- and 59-kDa polypeptides. However, since the study of Auguste *et al*. did not identify the position of incorporation of the various photoprobes into ^{125}I-apamin (α-Cys_1 or ϵ-Lys_4), it was not possible to directly correlate the structural properties of different azido photoprobes with their ability to label distinct polypeptides.

At present, the existing data from rat brain implicates the 86- and 33-kDa polypeptides as the best candidate subunits of neuronal SK_{Ca} channels, the other identified species being assigned as stable fragments derived from these parent structures (Leveque *et al*., 1990; Wadsworth *et al*., 1994). However, the unknown physiological relevance of the various fragments identified in brain (in particular the 59-kDa

† This research was supported by a project grant (37941) from the Wellcome Trust.

* Corresponding author.
‡ Hammersmith Hospital
§ University College London.

⊗ Abstract published in *Advance ACS Abstracts,* May 15, 1996.

[1] Abbreviations: BSA, bovine serum albumin; DSS, disuccinimido suberate; EDTA, ethylenediaminetetraacetic acid; EGTA, ethylene glycol bis(β-aminoethyl ether)-*N*,*N*,*N*′,*N*′-tetraacetic acid; HSAB, succinimido 4-azidobenzoate; SANPAA, succinimido [(4-azido-2-nitrophenyl)amino] acetate; SD, standard deviation; SDS−PAGE, sodium dodecyl sulfate−polyacrylamide gel electrophoresis; SK_{Ca} channels, small conductance Ca^{2+}-activated K^+ channels; sulfo-HSAB, sulfosuccinimido 4-azidobenzoate; sulfo-SANPAH, sulfosuccinimido 6-[(4-azido-2-nitrophenyl)amino]hexanoate; sulfo-SAPB, sulfosuccinimido 4-(4-azidophenyl)butyrate; tlc, thin-layer chromatography.

S0006-2960(96)00237-1 CCC: $12.00

polypeptide possibly representing a truncated form of the 86-kDa subunit) has led to proposals for heterooligomeric channel subtypes (Leveque *et al*., 1990). In addition, in the PC12 rat pheochromocytoma cell line (Auguste *et al*., 1989) or mammalian liver (Wadsworth *et al*., 1994), putative subtypes of apamin-sensitive SK_{Ca} channel have been identified on the basis of expression of distinct 25−30-kDa ^{125}I-apamin binding polypeptides that may replace the 33-kDa subunit found in neurons. These proposals for channel subtypes have now been supported at the functional level by recent findings showing that certain neuromuscular blockers differ in their ability to block neuronal and hepatic apamin-sensitive SK_{Ca} channels (Dunn *et al*., 1996).

In the present study, as a prerequisite for determining the heterooligomeric composition of putative SK_{Ca} channel subtypes, we have sought to define more precisely the structural criteria required to label different apamin-binding polypeptides expressed in brain and liver. In order to unambiguously couple azido photoprobes to either the α-Cys_1 or ϵ-Lys_4 amino groups of ^{125}I-apamin, we have synthesized, respectively, ^{125}I-[ϵ-formyl-Lys_4]apamin and ^{125}I-[α-formyl-Cys_1]apamin. Following the demonstration that both mono-^{125}I-[formyl]apamin derivatives retain high-affinity recognition of ^{125}I-apamin acceptor binding sites on rat brain membranes, we present the labeling patterns from rat brain synaptic membranes and rabbit liver plasma membranes obtained after coupling different photoprobes of variable spacer arm length in either the α- or ϵ-amino position of apamin. Results obtained from both tissues reveal stringent criteria for labeling high molecular mass (86- and 59-kDa) polypeptides, which are only accessible from the α-Cys_1 position using azido photoprobes of intermediate spacer arm length. A photoprobe of longer spacer arm length coupled in the α-Cys_1 position labels lower molecular mass polypeptides (around 30 kDa), as do all photoprobes (irrespective of spacer arm length) coupled through the ϵ-Lys_4 amino group. These data now provide the basis for rational interpretation of existing information regarding SK_{Ca} channel structure and indicate a close similarity in the topography of the apamin binding site present on pharmacologically distinct SK_{Ca} channel subtypes.

MATERIALS AND METHODS

Toxins and Chemicals. Native apamin was purified from *A. mellifera* bee venom as described previously (Strong & Brewster, 1992). Na^{125}I (carrier-free; [IMS 30]) was purchased from Amersham. Disuccinimido suberate (DSS) was purchased from Pierce, as were all azido succinimido ester photoprobes, with the exception of succinimido [(4-azido-2-nitrophenyl)amino]acetate (SANPAA), which was synthesized by the method of Ofengand *et al*. (1977). This compound is the same as that used by Seagar *et al*. (1985, 1986), but in the present study for the purposes of self-consistency with the nomenclature used for commercially available azido photoprobes, we have changed its acronym to SANPAA. The structures of these molecules together with their acronyms and IUPAC names are given in Figure 1. The acronyms referenced in the footnotes are based on nomenclature provided by the supplier. Protease inhibitors and bovine serum albumin (BSA, fraction V, protease-free) were purchased from Sigma. All other chemicals were of analytical grade.

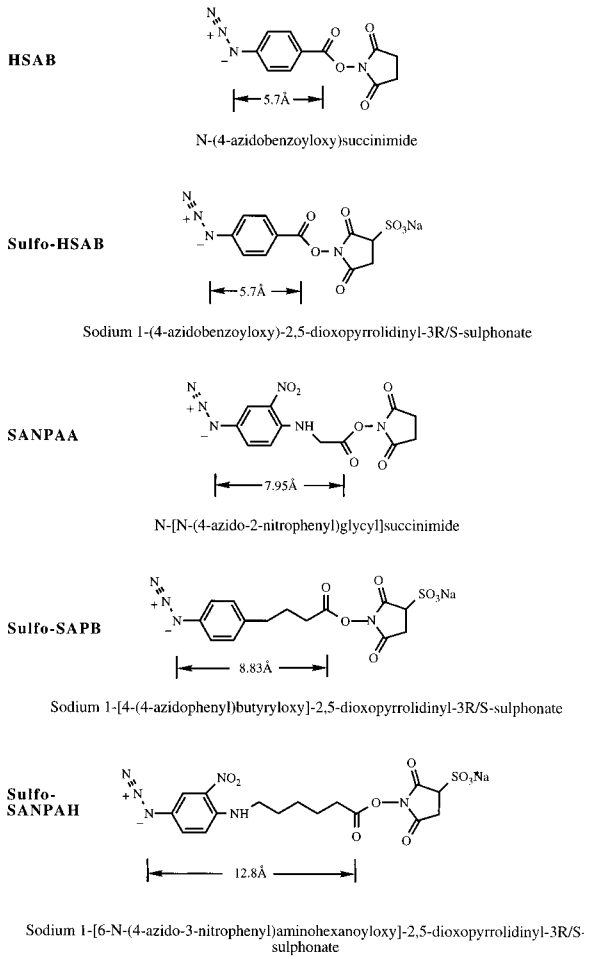

FIGURE 1: Structures of photolabile probes used in this study. For convenience each compound is identified by a chemical acronym based on earlier structural nomenclature (see Materials and Methods). For clarity the IUPAC name is also provided here. Following toxin derivatization and generation of photoreactive nitrene intermediates, the distances shown represent the maximum length of the bridging arm separating apamin from potential points of attachment within the acceptor binding site.

Formylation of Apamin. Procedures for the selective formylation of apamin at either the α-amino group of Cys_1 or the ϵ-amino group of Lys_4 were adapted from the original syntheses of Dempsey, (1982). *Preparation of [ϵ-formyl-Lys_4]apamin*: Apamin (4.3 mg, approximately 2 μmol) was dissolved in 0.75 mL of 0.1 M sodium borate buffer, pH 9.2, and cooled to 0 °C in an ice bath. 4-Nitrophenylformate (1.7 mg, 10 μmol, 5-fold molar excess) in 10 μL of dry tetrahydrofuran was added in two equal aliquots (at time zero and after 5 min). The reaction was allowed to proceed for a further 7 min (12 min total) and was then quenched with 4 × 20 μL of 2 M formic acid (until the yellow color of the nitrophenyl anion disappeared). After extraction of the reaction mixture with diethyl ether (3 × 750 μL), the aqueous phase was directly applied to an S-Sepharose (Pharmacia) cation-exchange column (8 cm × 1-cm diameter) equilibrated in 50 mM sodium acetate, pH 4.8. The column was eluted (flow rate 15 mL/h) with 3 column volumes of equilibration buffer and then with a linear gradient (120 mL) of 0−0.5 M NaCl developed in the same buffer. Eluate fractions (2 mL) were monitored at 254 nm. [ϵ-Formyl-Lys_4]apamin eluted at 0.35 M NaCl and its identity was confirmed by amino acid sequencing using an Applied Biosystems 477A sequencer. *Preparation of [α-Formyl-Cys_1]apamin*: Apamin

(6 mg, 3 μmol) was dissolved in 120 μL of formic acid (98%) and 10 × 2-μL aliquots of acetic anhydride were added at 30-s intervals with brief agitation between each addition; the final ratio of formic acid:acetic anhydride = 6:1 (v/v). Following gentle agitation at room temperature for a further 90 min, the reaction was diluted to 1 mL with distilled water and applied to an S-Sepharose cation-exchange column (8 cm × 1-cm diameter) equilibrated in 0.1 M sodium acetate, pH 4.7. The column was eluted (flow rate 15 mL/h) with 3 column volumes of equilibration buffer and then with a linear gradient (120 mL) of 0−0.5 M NaCl developed in the same buffer. Eluate fractions (1 mL) were monitored at 254 nm. [α-Formyl-Cys_1]apamin eluted at 0.24 M NaCl.

Radioiodination Procedures. Apamin was radioiodinated at His_{18} using a solid-phase Iodogen reaction and pure monoiodo-^{125}I-apamin (~2200 Ci/mmol) isolated by S-Sepharose cation-exchange chromatography as described previously (Strong & Brewster, 1992). [α-Formyl-Cys_1]-apamin and [ϵ-formyl-Lys_4]apamin were similarly iodinated at His_{18} using essentially the same reaction conditions. Briefly, ~50 μg of either formyl peptide (in sodium acetate buffer, pH ~4.8; see above) was adjusted (with appropriate aliquots of H_2O and 1.5 M Tris-HCl, pH 8.8) to pH ~8.6 and a final volume of 120 μL. Each peptide was then reacted with 37 MBq (1 mCi) of carrier-free $Na^{125}I$ (10 μl of 100 mCi/mL) for 20 min in the presence of 75 nmol of immobilized Iodogen (1,3,4,6-tetrachloro-3α,6α-diphenylglycouril, Sigma). Subsequently, the reaction was quenched by transfer of the sample into 5 mL of 10 mM sodium phosphate, pH 6.0, and adjustment of the final pH to ~5.5 by the addition of 200 μL of 100 mM acetic acid. Quenched reactions were then applied (at 0.5 mL/min) to an S-Sepharose cation-exchange column (5 cm × 1-cm diameter) equilibrated in 10 mM sodium phosphate, pH 6.0. Following the removal of free ^{125}I with 35 mL of equilibration buffer, monoiodo-^{125}I-[α-formyl-Cys_1]apamin or ^{125}I-[ϵ-formyl-Lys_4]-apamin (~2200 Ci/mmol) was isolated with a linear gradient of 0−200 mM NaCl developed in the same buffer. ^{125}I-[α-Formyl-Cys_1]apamin or ^{125}I-[ϵ-formyl-Lys_4]apamin eluted as a single peak at 140−160 mM NaCl. Unmodified [α-formyl-Cys_1]apamin and [ϵ-formyl-Lys_4]apamin eluted at higher salt concentrations (220−240 mM NaCl) and were routinely isolated at the end of the salt gradient by a stepwise increase in salt to 300 mM. Peak fractions of ^{125}I-[α-formyl-Cys_1]-apamin or ^{125}I-[ϵ-formyl-Lys_4]apamin identified from the gradient by γ-counting were pooled (to ~20 nM final concentration) and stored at 4 °C in the presence of 2 mg/mL BSA.

Preparation of Photolabile Derivatives of ^{125}I-[α-Formyl-Cys_1]apamin or ^{125}I-[ϵ-Formyl-Lys_4]apamin. All manipulations with azido succinimido ester photoprobes were performed in a darkroom under a 25-W photographic red lamp. Aliquots of ^{125}I-[α-formyl-Cys_1]apamin (in ~0.15 M NaCl and 10 mM sodium phosphate, pH 6.0, containing 2 mg/mL BSA) were diluted with an equal volume of 100 mM borax, pH 8.5, and incubated (at pH 8.5) with a 5−10-fold molar excess of succinimido ester photoprobes to primary reactive amines (present in ^{125}I-apamin and BSA) as detailed in legends to figures. Similarly, aliquots of ^{125}I-[ϵ-formyl-Lys_4]-apamin (in ~0.15 M NaCl and 10 mM sodium phosphate, pH 6.0, containing 2 mg/mL BSA) were diluted with an equal volume of 50 mM sodium phosphate, pH 6.0, and incubated (at pH 6.0) with a 10-fold molar excess of succinimido ester photoprobes to primary reactive amines (present in ^{125}I-apamin and BSA). For our purposes 50 lysine groups present in BSA were considered available to react with succinimido esters (Bernatowicz & Matsueda, 1986). Acetonitrile (100%) was used as a carrier for stock solutions of succinimido ester photoprobes, whereas 75% (v/v) acetonitrile prepared in H_2O was used for sulfosuccinimido ester photoprobes. In all cases reactions were allowed to proceed to completion by incubation in the dark for 3 h at 20 °C, after which photolabile products were stored in the dark at 4 °C and used within 24 h of preparation.

For simplicity, photolabile derivatives of ^{125}I-[α-formyl-Cys_1]apamin or ^{125}I-[ϵ-formyl-Lys_4]apamin are named on the basis of the modifying compound and the position of incorporation within the toxin molecule. For example ^{125}I-[α-formyl-Cys_1,ϵ-HSAB-Lys_4]apamin is the derivative formed after reaction of ^{125}I-[α-formyl-Cys_1]apamin with either HSAB or sulfo-HSAB.

Binding Assays. Binding of ^{125}I-apamin, ^{125}I-[α-formyl-Cys_1]apamin, or ^{125}I-[ϵ-formyl-Lys_4]apamin to purified rat brain cerebrocortical synaptic plasma membranes was performed using a filtration binding assay as described previously (Wadsworth *et al*., 1994). The incubation medium (1 mL) consisted of 10 mM KCl and 25 mM Tris-HCl, pH 8.4, containing 0.1% (w/v) BSA. In saturation experiments, aliquots (40−60 μg of protein) of purified plasma membranes were incubated with increasing concentrations of each ^{125}I-labeled species in the absence or presence of 0.1 μM unlabeled apamin. The standard deviation of the means were typically between 3% and 5% in triplicate assays. Results from saturation experiments were examined by Scatchard analysis and site-fitting using the computer programs EBDA and LIGAND (Biosoft, Cambridge, U.K.). Semilogarithmic plots of saturable binding against free ^{125}I-ligand concentration were sigmoidal, thereby confirming the reliable determination of the equilibrium dissociation constant (K_d) and maximum acceptor concentration (B_{max}).

Photolabeling Procedures. Cerebrocortical synaptic plasma membranes or hepatic plasma membranes (Wadsworth *et al*., 1994), were resuspended in 10 mM KCl and 25 mM borax, pH 9.0, containing 1 mM 4-(2-aminoethyl)benzenesulfonyl fluoride, 1 mM EDTA, 0.1 mM iodoacetamide, and 0.1% (w/v) BSA. Aliquots (1 mL, containing ~0.5 mg of membrane protein) were incubated for 1 h on ice in the dark with 100 pM of the various azido photoprobe derivatives of ^{125}I-[α-formyl-Cys_1]apamin and ^{125}I-[ϵ-formyl-Lys_4]apamin in the absence or presence of 0.1 μM native apamin as detailed in legends to figures. Membranes were subsequently sedimented by centrifugation (20000*g*, 5 min, 4 °C) and, following aspiration of the supernatant, resuspended in 1 mL of ice-cold borax/KCl buffer containing protease inhibitors but lacking BSA. Membrane suspensions were then immediately irradiated on ice for 20 min at ~1−2 cm from a 25-W long-wave UV lamp (λ_{max} = 366 nm). Following their recovery by centrifugation (as above), membrane pellets were washed once with 1 mL of ice-cold borax/KCl buffer containing protease inhibitors and then snap-frozen in liquid N_2. Cross-linking experiments using the homobifunctional reagent DSS were performed as described previously (Wadsworth *et al*., 1994).

Thin-Layer Chromatography. Thin-layer chromatography (tlc) was routinely used as a convenient method of assessing the reaction of succinimido ester photoprobes with ^{125}I-

[formyl]apamin. Selective modification of primary amines within apamin leads to a loss of positive charge and results in an increased chromatographic mobility (Dempsey, 1982). Briefly, ^{125}I-apamin derivatives (~3 μL containing ~25−50 fmol/lane) were applied to cellulose K2 tlc plates (250 μm, 10 × 20 cm; Whatman International) and developed in a solvent system of 3:3:3:1 (v/v/v/v) butan-1-ol:pyridine:water:acetic acid (Habermann & Fischer, 1979). Radioactivity was visualized by exposing the dried plates to X-ray film for up to 12 h using an intensifying screen.

Polyacrylamide Gel Electrophoresis. SDS sample buffer consisted of 20 mM Tris-HCl, pH 6.8, containing 4% (w/v) SDS, 10% (v/v) glycerol, 2 mM EDTA, 2 mM EGTA, 10 μg/mL soybean trypsin inhibitor, 0.2 mM benzamidine, 0.1 mM phenylmethanesulfonyl fluoride, 5 μM pepstatin A, 1 mM iodoacetamide, 10 μM leupeptin, 1 mM 1,10-phenanthroline, and 25 μg/mL bacitracin. Samples were denatured in SDS sample buffer by heating at 95 °C for 5 min under reducing or nonreducing conditions in the presence or absence, respectively, of 5% (v/v) 2-mercaptoethanol. Aliquots (up to 100 μg of protein) were analyzed by discontinuous SDS−PAGE (Laemmli, 1970) using gradient gels as detailed in legends to figures. Radioactive bands were identified by exposing the dried gel to X-ray film (Hyperfilm-MP; Amersham) using an intensifying screen. Molecular masses of ^{125}I-apamin-labeled polypeptides were determined by comparison to the migration of known standards and are reported following the subtraction of 2 kDa, which represents the approximate molecular mass contributed by ^{125}I-apamin.

RESULTS

Preparation and Characterization of ^{125}I-[α-Formyl-Cys$_1$]-apamin and ^{125}I-[ϵ-Formyl-Lys$_4$]apamin. In order to specifically attach amine-directed succinimido ester azido photoprobes to either the α-amino or the ϵ-amino group of apamin, we first sought to prepare two precursor neurotoxin derivatives chemically blocked at one or the other position. We chose to prepare [formyl]apamin derivatives since they have been previously synthesized (Dempsey, 1982) and this modification introduces minimal steric bulk at the derivatized amino group. Formylation of apamin with *p*-nitrophenyl formate at alkaline pH, and separation of the reaction mixture by cation-exchange chromatography, resulted in the isolation of [ϵ-formyl-Lys$_4$]apamin from di-formyl[α-Cys$_1$,ϵ-Lys$_4$]-apamin and unmodified apamin (Figure 2A). The identity of [ϵ-formyl-Lys$_4$]apamin (as assigned from its chromatographic elution position) was confirmed by amino acid sequencing, which verified exclusive block of the ϵ-amino group of Lys$_4$. Formylation of the α-amino group of apamin was achieved by treating the toxin with acetic anhydride in formic acid. Under these highly acidic conditions the concentration of the nucleophilic (unprotonated) form of the ϵ-amino group is extremely low, thereby favoring formylation of the α-amino group (Dempsey, 1982). Separation of this reaction mixture, using conditions analogous to those used earlier, resulted in pure [α-formyl-Cys$_1$]apamin being recovered in high yield (~90%) from only trace contaminants of diformyl[α-Cys$_1$,ϵ-Lys$_4$]apamin and unmodified apamin (data not shown). Subsequently, both [α-formyl-Cys$_1$]-apamin and [ϵ-formyl-Lys$_4$]apamin were radioiodinated using slight modifications of the solid-phase radioiodination procedures used to prepare ^{125}I-apamin (Strong & Brewster,

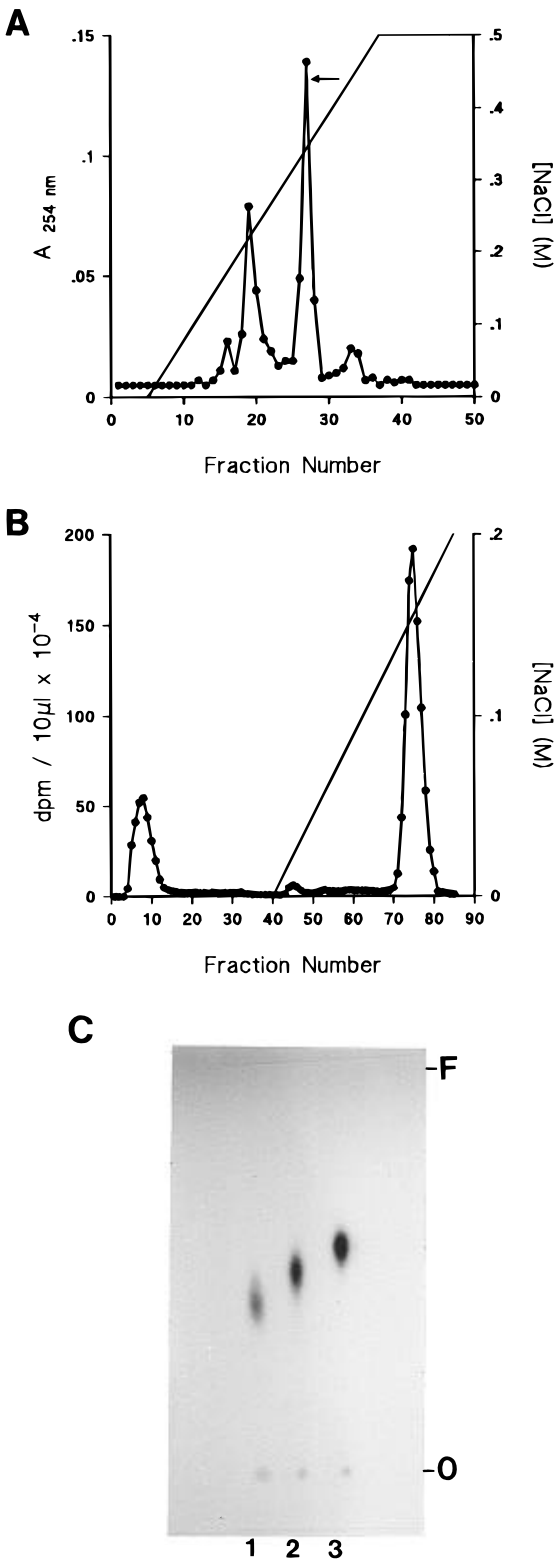

FIGURE 2: Preparation and radioiodination of [ϵ-formyl-Lys$_4$]-apamin. (A) Apamin was derivatized with 4-nitrophenyl formate at pH 9.2 and the reaction products were separated on an S-Sepharose column at pH 4.8 using a NaCl gradient as described under Materials and Methods. The elution position of [ϵ-formyl-Lys$_4$]-apamin is indicated by the arrow. (B) [ϵ-formyl-Lys$_4$]apamin was radiolabeled with Na^{125}I and the reaction products were separated on an S-Sepharose column at pH 6.0 using a NaCl gradient as described under Materials and Methods. Monoiodo ^{125}I-[ϵ-formyl-Lys$_4$]apamin eluted at ~0.15 M NaCl. (C) Analysis of ^{125}I-apamin derivatives by tlc (solvent system 3:3:3:1 (v/v/v/v) butan-1-ol:pyridine:H$_2$O:acetic acid). (Lane 1) ^{125}I-apamin; (lane 2) ^{125}I-[α-formyl-Cys$_1$]apamin; (lane 3) ^{125}I-[ϵ-formyl-Lys$_4$]apamin. The positions of the origin (O) and solvent front (F) are as shown. Radioactivity was visualized by exposing the dried tlc plate to X-ray film.

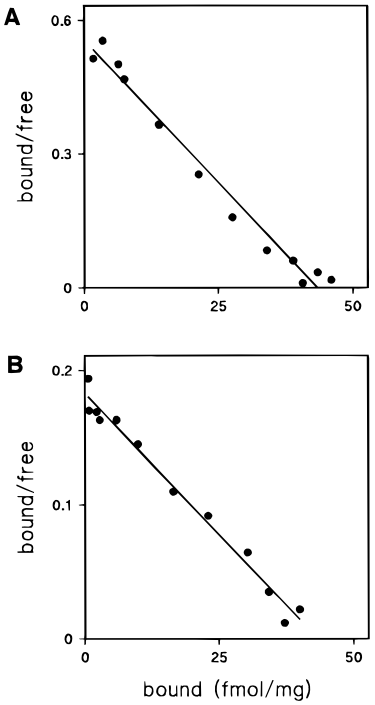

FIGURE 3: Binding of ^{125}I-[formyl]apamin derivatives to rat brain plasma membranes. Rat brain synaptic plasma membranes (40−60 μg of protein/mL) were incubated with increasing concentrations (0.2−150 pM) of ^{125}I-[α-formyl-Cys_1]apamin (A) or ^{125}I-[ϵ-formyl-Lys_4]apamin (B) in the absence or presence of 0.1 μM native apamin. The binding medium consisted of 10 mM KCl and 25 mM Tris-HCl, pH 8.4, containing 0.1% (w/v) BSA. Following equilibration on ice for 1 h, membranes were analyzed using a filtration assay. Saturable binding is presented in the form of Scatchard plots. The results are given in the text. The figures presented are typical of results obtained with three different preparations of rat brain membranes.

1992). Both ^{125}I-[ϵ-formyl-Lys_4]apamin (Figure 2B) or ^{125}I-[α-formyl-Cys_1]apamin (not shown) were similarly isolated as single peaks from cation-exchange chromatography, which migrated as single homogeneous spots when analyzed by tlc (Figure 2C). Consistent with the behavior of the noniodinated peptides (Dempsey, 1982), ^{125}I-[formyl]apamin derivatives migrated with increased mobility relative to ^{125}I-apamin, the rank order of mobility being ^{125}I-[ϵ-formyl-Lys_4]-apamin > ^{125}I-[α-formyl-Cys_1]apamin > ^{125}I-apamin (Figure 2C).

Both ^{125}I-[α-formyl-Cys_1]apamin and ^{125}I-[ϵ-formyl-Lys_4]-apamin were found to retain high-affinity recognition of ^{125}I-apamin acceptor binding sites on rat brain cerebrocortical synaptosomes (Figure 3). Using membrane preparations displaying single classes of high-affinity ^{125}I-apamin binding sites ($K_d = 3.3 \pm 0.8$ pM, B_{max} 47 ± 6 fmol/mg of membrane protein; SD $n = 4$) (not shown), ^{125}I-[α-formyl-Cys_1]apamin displayed almost identical binding affinity ($K_d = 3.9 \pm 0.5$ pM, SD $n = 3$), while ^{125}I-[ϵ-formyl-Lys_4]apamin recognized the same sites with slightly reduced affinity ($K_d = 11.9 \pm 0.9$ pM, SD $n = 3$). Student's *t*-test analysis revealed that the difference between the binding affinities of ^{125}I-apamin and ^{125}I-[α-formyl-Cys_1]apamin was not statistically significant ($p > 0.25$), whereas the difference between the affinities of ^{125}I-apamin and ^{125}I-[ϵ-formyl-Lys_4]apamin, although small, was nevertheless statistically significant ($p < 0.01$). These results are largely consistent with those of others (Vincent *et al*., 1975; Seagar *et al*., 1986), who similarly reported minimal perturbation of apamin's activity following modification of either of the toxin's two primary amines.

Preparation of Photolabile Derivatives of ^{125}I-[α-Formyl-Cys_1]apamin and ^{125}I-[ϵ-Formyl-Lys_4]apamin. In accordance with earlier findings (Seagar *et al*., 1986), the ϵ-amino group of apamin was found to react efficiently with succinimido ester photoprobes. Tlc analysis of the reaction of ^{125}I-[α-formyl-Cys_1]apamin at pH 8.5 with an excess of sulfo-HSAB, SANPAA, sulfo-SAPB, or sulfo-SANPAH (see Figure 1 for structures) revealed complete conversion of the starting toxin to the corresponding ϵ-photolabile derivative (Figure 4A). Homogeneous ϵ-photolabile derivatives of ^{125}I-[α-formyl-Cys_1]apamin were routinely prepared in this manner and subsequently used in photolabeling experiments described below. In contrast to the ease of derivatization of the ϵ-amino group, similar derivatization of the α-amino group

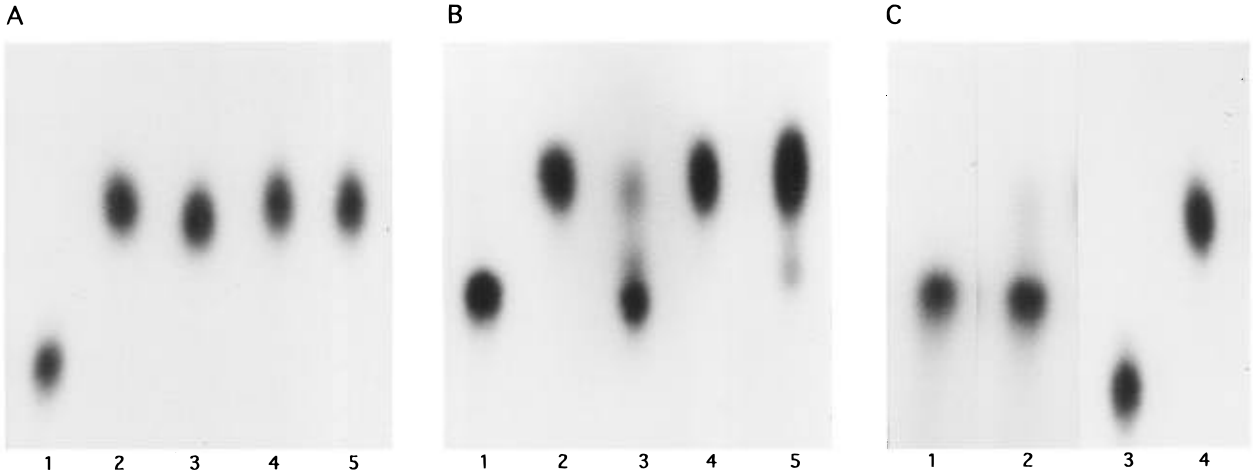

FIGURE 4: Tlc analysis of the reaction of ^{125}I-[formyl]apamin derivatives with succinimido ester photoprobes. ^{125}I-[α-Formyl-Cys_1]apamin or ^{125}I-[ϵ-formyl-Lys_4]apamin were incubated with various succinimido ester photoprobes as described under Materials and Methods. Equivalent aliquots (~25 fmol) of the starting ligand and reaction products were analyzed by tlc and visualized by autoradiography of the dried plates. (A) ^{125}I-[α-Formyl-Cys_1]apamin before (lane 1) and after reaction with a 10-fold molar excess of sulfo-HSAB (lane 2), SANPAA (lane 3), sulfo-SAPB (lane 4), or sulfo-SANPAH (lane 5). (B) ^{125}I-[ϵ-Formyl-Lys_4]apamin before (lane 1) and after reaction with a 10-fold molar excess of sulfo-HSAB (lane 2), SANPAA (lane 3), sulfo-SAPB (lane 4), or sulfo-SANPAH (lane 5). (C) ^{125}I-[ϵ-Formyl-Lys_4]apamin before (lane 1) and after (lane 2) reaction with a 5-fold molar excess of HSAB; ^{125}I-[α-formyl-Cys_1]apamin before (lane 3) and after (lane 4) reaction with a 5-fold molar excess of HSAB.

was not as straightforward. In preliminary experiments conducted at pH 8.5, a 10-fold molar excess of sulfo-SAPB to primary reactive amines present in ^{125}I-[ϵ-formyl-Lys$_4$]-apamin and BSA produced only ~50% conversion of ^{125}I-[ϵ-formyl-Lys$_4$]apamin to the α-derivative (data not shown). Complete derivatization of ^{125}I-[ϵ-formyl-Lys$_4$]apamin, using the same molar excess of sulfo-SAPB, was, however, achieved by conducting the reaction at pH 6.0 (Figure 4B). At this lower pH the increased efficiency of coupling at the α-amino group may reflect reductions in both the rate of hydrolysis of the succinimido ester bond and in the reactivity of the ϵ-amino groups present in the carrier protein. These conditions were found to be equally effective for coupling sulfo-HSAB, sulfo-SAPB, or sulfo-SANPAH to ^{125}I-[ϵ-formyl-Lys$_4$]apamin (Figure 4B) and were routinely used in preparing these α-derivatives for use in photolabeling experiments. Surprisingly, under the same conditions SANPAA was found to react less efficiently with ^{125}I-[ϵ-formyl-Lys$_4$]apamin (Figure 4B). Typically, only 10−30% conversion of ^{125}I-[ϵ-formyl-Lys$_4$]apamin to the α-SANPAA derivative was achieved. This relatively low efficiency of incorporation could not readily be improved by increasing or decreasing the pH of the reaction (to either pH 8.5 or 5.0), by increasing the concentration of SANPAA, or by changing the organic solvent from acetonitrile to dimethyl sulfoxide (data not shown). Upon further investigation, it was discovered that when HSAB (rather than sulfo-HSAB) was reacted with ^{125}I-[ϵ-formyl-Lys$_4$]apamin, low levels of incorporation were obtained that were similar to that observed with SANPAA (Figure 4C). However, in accord with the efficient reaction of SANPAA with the ϵ-amino group, HSAB was found to react efficiently with ^{125}I-[α-formyl-Cys$_1$]apamin (Figure 4C). On the basis of these findings, no further attempt was made to improve the incorporation of SANPAA into ^{125}I-[ϵ-formyl-Lys$_4$]apamin and partially derivatized preparations containing ~20% ^{125}I-[α-SANPAA-Cys$_1$,ϵ-formyl-Lys$_4$]apamin were used in photolabeling experiments.

Photolabeling from the α-Cys$_1$ Position of Apamin. In agreement with the original findings of Seagar *et al*., (1986), photolabeling experiments using preparations of ^{125}I-[α-SANPAA-Cys$_1$,ϵ-formyl-Lys$_4$]apamin on rat brain synaptic plasma membranes resulted in the saturable incorporation of radioactivity into polypeptides of 86- and 59-kDa (Figure 5, lanes 3 and 4). The same polypeptides were also intensely labeled by ^{125}I-[α-SAPB-Cys$_1$,ϵ-formyl-Lys$_4$]apamin (Figure 5, lanes 5 and 6). While the use of a homogeneous preparation of the latter derivative versus a mixed preparation of ^{125}I-[α-SANPAA-Cys$_1$,ϵ-formyl-Lys$_4$]apamin and unmodified ^{125}I-[ϵ-formyl-Lys$_4$]apamin may account for gross differences in the intensities of labeling, the intensities of the 86- and 59-kDa polypeptides relative to each other were the same using either α-derivative. Additional weak labeling of a ~44-kDa component previously detected by Seagar *et al*. (1986) was also observed using ^{125}I-[α-SAPB-Cys$_1$,ϵ-formyl-Lys$_4$]apamin (Figure 6, lane 1). SANPAA and sulfo-SAPB therefore exhibit the same pattern of labeling when coupled through the α-amino group of ^{125}I-[ϵ-formyl-Lys$_4$]-apamin. The fact that both probes label the same 86- and 59-kDa polypeptides when coupled at the α-amino group suggests that structural differences between these two probes (see Figure 1), and in particular any contribution of electron-withdrawing substituents on the activity of photogenerated aromatic nitrene intermediates, have little effect on determining the specificity of labeling polypeptides within the apamin acceptor site.

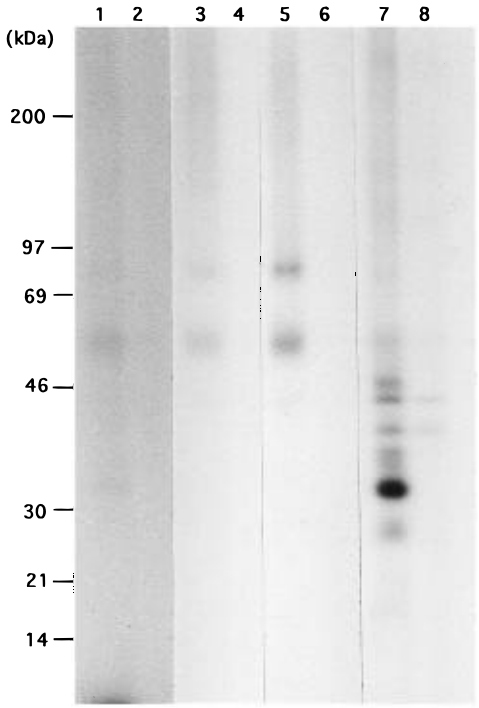

FIGURE 5: Autoradiogram of rat brain synaptic plasma membranes photolabeled from the α-Cys$_1$ position of apamin. Synaptic plasma membranes from rat brain were equilibrated with 100 pM ^{125}I-[α-HSAB-Cys$_1$,ϵ-formyl-Lys$_4$]apamin (lanes 1 and 2), 100 pM ^{125}I-[α-SANPAA-Cys$_1$,ϵ-formyl-Lys$_4$]apamin/^{125}I-[ϵ-formyl-Lys$_4$]-apamin (lanes 3 and 4), 100 pM ^{125}I-[α-SAPB-Cys$_1$,ϵ-formyl-Lys$_4$]-apamin (lanes 5 and 6) and 100 pM ^{125}I-[α-SANPAH-Cys$_1$,ϵ-formyl-Lys$_4$]apamin (lanes 7 and 8) in the absence (odd-numbered lanes) or presence (even-numbered lanes) of 0.1 μM native apamin. Following washing and photolysis as described under Materials and Methods, aliquots of each sample (~100 μg of protein) were analyzed by gradient pore [4−20% (w/v) acrylamide] SDS−PAGE run under reducing conditions.

In a subsequent series of experiments, the effect of varying the length of the spacer arm from the α-amino group was examined. Reducing the number of -CH_2- groups in the spacer arm through the use of ^{125}I-[α-HSAB-Cys$_1$,ϵ-formyl-Lys$_4$]apamin significantly compromised this derivative's ability to label the 86- and 59-kDa polypeptides. Only after prolonged exposure of autoradiograms (~10-fold longer than required for ^{125}I-[α-SAPB-Cys$_1$,ϵ-formyl-Lys$_4$]apamin) was weak saturable incorporation of radioactivity into these polypeptides detected (Figure 5, lanes 1 and 2). The efficiency of incorporation was not improved by altering the source of radiation for photolysis from 366 to 254 nm. These results were obtained using homogeneous preparations of ^{125}I-[α-HSAB-Cys$_1$,ϵ-formyl-Lys$_4$]apamin (see Figure 4B), whose levels of saturable binding to rat brain membranes (as measured by γ-counting) were equivalent to those obtained with ^{125}I-[α-SAPB-Cys$_1$,ϵ-formyl-Lys$_4$]apamin (data not shown). Inefficient labeling cannot therefore be attributed to a reduction in the capacity of ^{125}I-[α-HSAB-Cys$_1$,ϵ-formyl-Lys$_4$]apamin to recognize apamin acceptor binding sites. Furthermore, the low levels of incorporation observed with sulfo-HSAB in the α-amino position do not seem to be due to inefficient generation of photoreactive nitrene intermediates, as the same photolysis conditions produced strong photoaffinity labeling when sulfo-HSAB was coupled at the

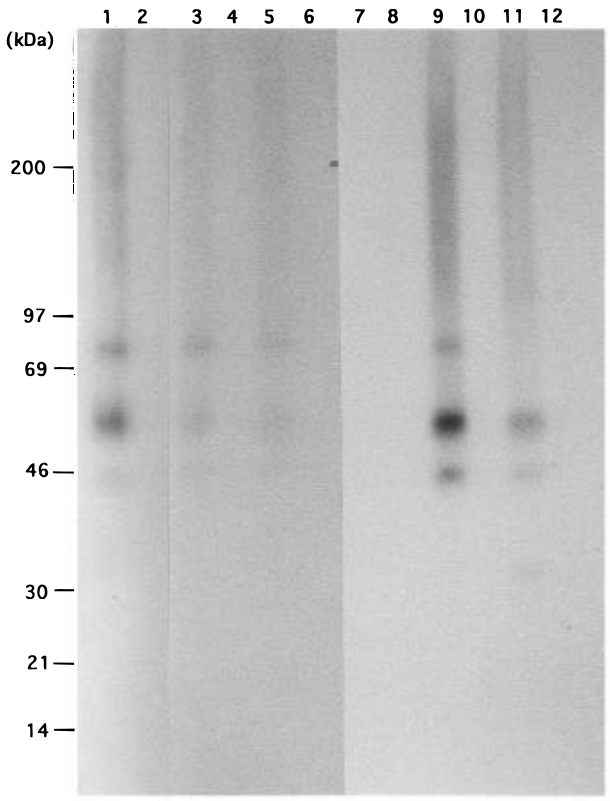

FIGURE 6: Autoradiogram of brain and liver plasma membranes from various species photolabeled with ^{125}I-[α-SAPB-Cys_1,ϵ-formyl-Lys_4]apamin. Plasma membranes from rat brain (lanes 1 and 2), guinea pig brain (lanes 3 and 4), rabbit brain (lanes 5 and 6), rat liver (lanes 7 and 8), guinea pig liver (lanes 9 and 10), and rabbit liver (lanes 11 and 12) were equilibrated with 100 pM ^{125}I-[α-SAPB-Cys_1,ϵ-formyl-Lys_4]apamin in the absence (odd-numbered lanes) or presence (even-numbered lanes) of 0.1 μM native apamin. After washing and photolysis, aliquots of each sample (∼100 μg of protein) were analyzed by gradient pore [4−20% (w/v) acrylamide] SDS−PAGE run under reducing conditions.

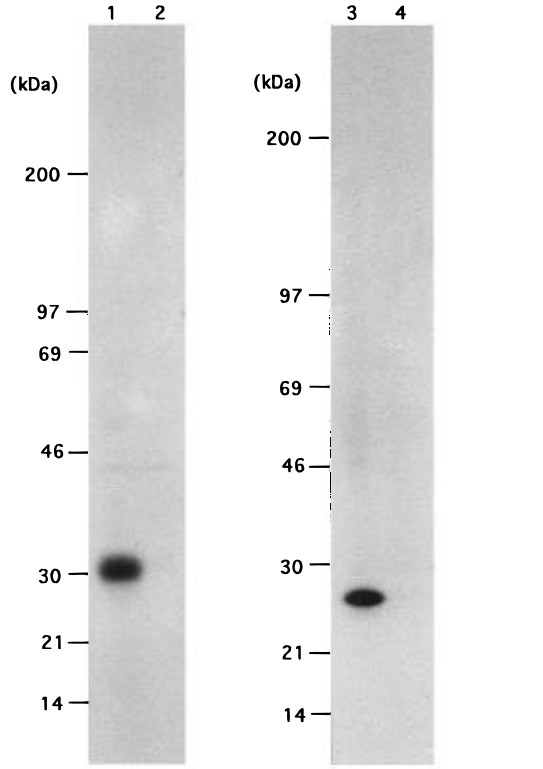

FIGURE 7: Autoradiogram of rabbit liver plasma membranes photolabeled with ^{125}I-[α-SANPAH-Cys_1,ϵ-formyl-Lys_4]apamin. Rabbit liver plasma membranes were equilibrated with 100 pM of ^{125}I-[α-SANPAH-Cys_1,ϵ-formyl-Lys_4]apamin in the absence (lanes 1 and 3) or presence (lanes 2 and 4) of 0.1 μM native apamin. Following washing and photolysis, aliquots of each sample (∼100 μg of protein) were analyzed by gradient pore [4−20% (w/v) acrylamide] SDS−PAGE run under reducing (lanes 1 and 2) or nonreducing (lanes 3 and 4) conditions.

ϵ-amino group of ^{125}I-[α-formyl-Cys_1]apamin (see below). For these reasons, it appears that efficient photolabeling of the 86- and 59-kDa apamin binding polypeptides can only be achieved when the azido group is attached at a distance >5.7 Å from the α-amino group.

Extension of the spacer arm to a maximum of 12.8 Å through the use of ^{125}I-[α-SANPAH-Cys_1,ϵ-formyl-Lys_4]-apamin yielded a surprising result, and it appears that a distinct upper limit to the length of the spacer arm separating the azido group from the α-amino group of apamin may also govern labeling of the 86- and 59-kDa polypeptides. Instead of labeling the 86- and 59-kDa polypeptides, ^{125}I-[α-SANPAH-Cys_1,ϵ-formyl-Lys_4]apamin was saturably incorporated into the 33-kDa apamin binding polypeptide present on rat brain synaptic plasma membranes (Figure 5, lanes 7 and 8). (It should be noted that this particular ligand appeared to be rather "sticky"; nonspecific binding levels were ∼2−3-fold higher than found with other α-photolabile derivatives and some nonspecific labeling was observed.) Given that the structures of toxin derivatives after treatment with SANPAA and SANPAH are identical, except for the number of methylene bridging groups (one versus five -CH_2- groups) (Figure 1), our data indicate that the ability to label either the 86- and 59-kDa or the 33-kDa apamin binding polypeptides from the α-amino group of apamin is dependent upon the length of the spacer arm incorporated into the photoprobe. The patterns of labeling presented here were reproduced with three preparations of rat brain plasma membranes, and in agreement with earlier findings (Seagar *et al*., 1986), none of the labeled polypeptides showed any significant change in mobility following electrophoresis under nonreducing conditions (data not shown).

Having demonstrated that the length of spacer arm in α-azido derivatives of ^{125}I-[ϵ-formyl-Lys_4]apamin influences the ability of these ligands to label high or low molecular mass polypeptides associated with neuronal SK_{Ca} channels, we then wished to see if this was also the case in labeling analogous polypeptides associated with SK_{Ca} channels in mammalian liver. Rabbit and guinea pig liver are believed to contain putative subtypes of SK_{Ca} channel that can be distinguished on the basis of expression of distinct 25−30-kDa apamin binding polypeptides (Wadsworth *et al*., 1994). In initial experiments using ^{125}I-[α-SAPB-Cys_1,ϵ-formyl-Lys_4]apamin, we first sought to compare the expression of high molecular mass apamin binding polypeptides present on plasma membranes from either the brain or liver of these two species. The pattern of labeling of 86-, 59-, and 44-kDa polypeptides from guinea pig and rabbit brain was found to be virtually identical to that observed on rat brain membranes (Figure 6, lanes 1−6). Although the intensity of labeling on guinea pig and rabbit brain plasma membranes was lower than that found with rat brain, this is in good correlation with the lower site densities of ^{125}I-apamin acceptors present on these preparations (Wadsworth *et al*., 1994). In contrast to the findings in brain, differences in

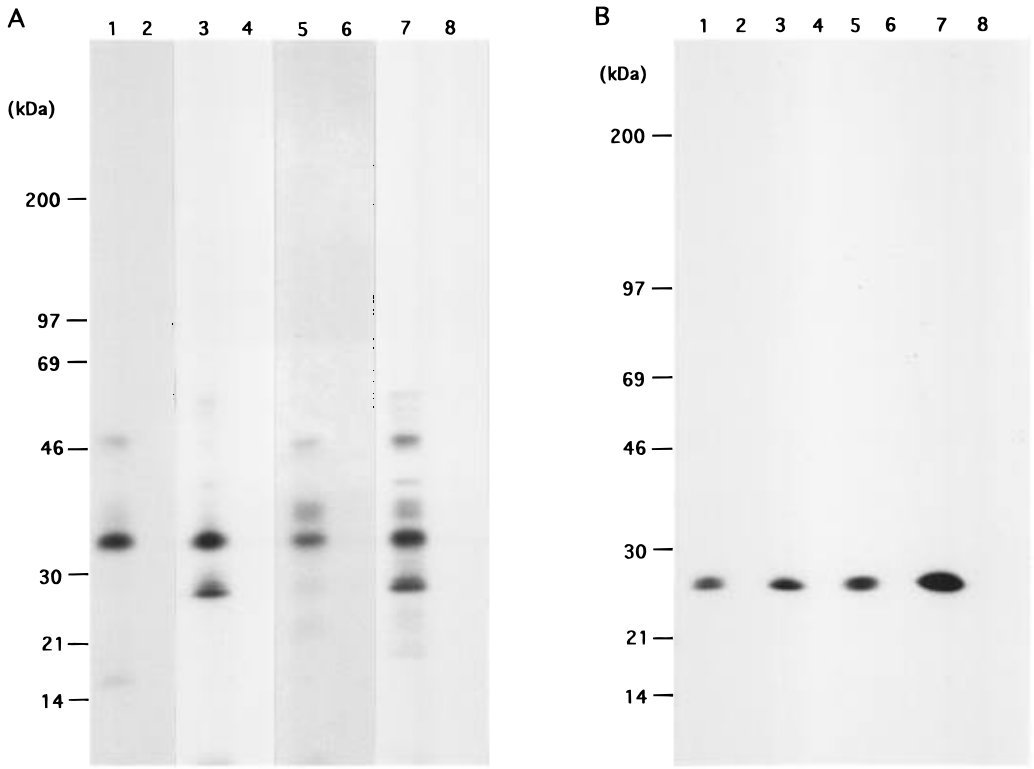

FIGURE 8: Autoradiogram of rat brain and rabbit liver plasma membranes photolabeled from the ϵ-Lys$_4$ position of apamin. Rat brain synaptic plasma membranes (A) or rabbit liver plasma membranes (B) were equilibrated with 100 pM of either ^{125}I-[α-formyl-Cys$_1$,ϵ-HSAB-Lys$_4$]apamin (lanes 1 and 2), ^{125}I-[α-formyl-Cys$_1$,ϵ-SANPAA-Lys$_4$]apamin (lanes 3 and 4), ^{125}I-[α-formyl-Cys$_1$,ϵ-SAPB-Lys$_4$]apamin (lanes 5 and 6), or ^{125}I-[α-formyl-Cys$_1$,ϵ-SANPAH-Lys$_4$]apamin (lanes 7 and 8) in the absence (odd-numbered lanes) or presence (even-numbered lanes) of 0.1 μM native apamin. Following washing and photolysis, aliquots of each sample ($\sim$100 μg of protein) were analyzed by gradient pore [4−20% (w/v) acrylamide] SDS−PAGE run under reducing (A) or nonreducing (B) conditions.

the expression of the 86- and 59-kDa polypeptides were observed on liver plasma membranes. In correlation with the reported absence of functional apamin-sensitive SK$_{Ca}$ channels in rat liver (Takanashi *et al*., 1992), ^{125}I-[α-SAPB-Cys$_1$,ϵ-formyl-Lys$_4$]apamin did not label any polypeptides on rat liver plasma membranes (Figure 6, lanes 7 and 8). However, consistent with the findings of Marqueze *et al*. (1987), labeling of guinea pig liver plasma membranes with ^{125}I-[α-SAPB-Cys$_1$,ϵ-formyl-Lys$_4$]apamin identified 86-, 59-, and 44-kDa polypeptides indistinguishable from those observed in brain (Figure 6, lanes 9 and 10). On rabbit liver plasma membranes only the 59-kDa polypeptide was detected, accompanied by weaker labeling of the 44-kDa polypeptide and the previously detected 30-kDa apamin binding polypeptide (Figure 6, lanes 11 and 12) (Wadsworth *et al*., 1994). This pattern of labeling was reproduced with three preparations of rabbit liver membranes and was also obtained (with reduced intensities) using ^{125}I-[α-SANPAA-Cys$_1$,ϵ-formyl-Lys$_4$]apamin or ^{125}I-[α-HSAB-Cys$_1$,ϵ-formyl-Lys$_4$]apamin (data not shown). Although highly selective proteolysis cannot be unequivocally ruled out, it appears that negligible levels of the 86-kDa apamin binding polypeptide are expressed on rabbit hepatocytes (see discussion). In exactly the same manner as was seen with rat brain plasma membranes, photolabeling of rabbit liver plasma membranes with ^{125}I-[α-SANPAH-Cys$_1$,ϵ-formyl-Lys$_4$]apamin produced a switch from labeling the high molecular mass 59-kDa polypeptide to labeling the 30-kDa polypeptide (Figure 7, lanes 1 and 2). Under nonreducing conditions this polypeptide migrated with an apparent molecular mass of 25 kDa (Figure 7, lane 3), which is in accordance with our previous observations obtained after coupling ^{125}I-apamin with DSS (Wadsworth *et al*., 1994). Since this anomalous electrophoretic behavior is apparent after labeling with a specific photolabile probe, the phenomenon cannot be attributed to an artifact arising from the use of a homobifunctional cross-linker.

The present findings suggest significant similarity in the organization of polypeptide subunits comprising tissue-specific subtypes of an apamin-sensitive SK$_{Ca}$ channel. Moreover, because the topography of the apamin acceptor binding site appears to be conserved between channel subtypes, we are now able to propose general criteria that must be fulfilled in order to label specific channel-associated polypeptides from the α-amino position of the toxin. Assuming to a first approximation that spacer arm length is based on the methylene bridging groups occupying a fully extended conformation, our findings indicate that an $\sim$8−9-Å separation of the azido group from the α-amino group is required for optimal labeling of the 86- and 59-kDa polypeptides. Shortening this distance reduces the efficiency of labeling of these polypeptides, whereas an increase in spacer arm length restricts labeling of the high molecular mass polypeptides and favors labeling of the smaller $\sim$30-kDa subunits.

Photolabeling from the ϵ-Lys$_4$ Position of Apamin. In contrast to the patterns of labeling obtained from the α-amino group of apamin, all ϵ-azido derivatives of ^{125}I-[α-formyl-Cys$_1$]apamin were strongly and saturably incorporated into the 33-kDa apamin binding polypeptide present on rat brain synaptic plasma membranes (Figure 8A). Although ϵ-derivatives also weakly labeled a 46-kDa polypeptide, incor-

poration into the higher molecular mass 86- and 59-kDa apamin binding polypeptides was not detected from the ϵ-amino position. In addition to the intense labeling of the 33-kDa polypeptide, all ϵ-azido derivatives also saturably labeled doublets of polypeptides around 36 or 22−24 kDa. However the relative incorporation of radioactivity into these components varied between each ϵ-derivative. ^{125}I-[α-formyl-Cys_1,ϵ-SANPAA-Lys_4]apamin and ^{125}I-[α-formyl-Cys_1,ϵ-SANPAH-Lys_4]apamin produced the highest intensity of labeling of the doublet of polypeptides of ~22−24 kDa, whereas ^{125}I-[α-formyl-Cys_1,ϵ-SAPB-Lys_4]apamin and ^{125}I-[α-formyl-Cys_1,ϵ-SANPAH-Lys_4]apamin were most efficient in labeling the doublet of polypeptides of ~36 kDa (Figure 8A). These findings complement those of Seagar *et al*. (1986), who also detected the same polypeptides using ^{125}I-[ϵ-SANPAA-Lys_4]apamin. As expected, no significant change in the mobility of the polypeptides labeled in brain was observed after electrophoresis under nonreducing conditions (data not shown). Although at present we are unable to shed any further light on a potential structural role for the ~36- or 22-kDa polypeptides within neuronal SK_{Ca} channels, these polypeptides were not detected on liver membranes. Indeed, all ϵ-azido derivatives of ^{125}I-[α-formyl-Cys_1]apamin (irrespective of the length of spacer arm) were incorporated exclusively into the 30-kDa apamin binding polypeptide present on rabbit liver plasma membranes, which was readily distinguished by its migration as a ~25-kDa species in the absence of reducing agent (Figure 8B). The observation that ϵ-azido derivatives of ^{125}I-[α-formyl-Cys_1]-apamin are only incorporated into low molecular mass polypeptides on both brain and liver plasma membranes reaffirms the notion that the topography of the neurotoxin binding site is similarly conserved within tissue-specific subtypes of SK_{Ca} channel.

Cross-Linking of ^{125}I-[α-Formyl-Cys_1]apamin or ^{125}I-[ϵ-Formyl-Lys_4]apamin Using Disuccinimido Suberate. It has been widely established that ^{125}I-apamin is incorporated into ~30-kDa apamin binding polypeptides following cross-linking to its acceptors using DSS (Hugues *et al*., 1982b; Schmid-Antomarchi *et al*., 1984; Auguste *et al*., 1989; Wadsworth *et al*., 1994). However, the relative participation of ^{125}I-apamin's two free amino groups in DSS-mediated coupling has not been established. The availability of ^{125}I-[α-formyl-Cys_1]apamin and ^{125}I-[ϵ-formyl-Lys_4]apamin enabled us to directly evaluate the contribution of the α- and ϵ-amino groups of apamin in such reactions. Following equilibrium binding of either ^{125}I-[formyl]apamin derivative to rat brain synaptic plasma membranes or rabbit liver plasma membranes, and subsequent exposure to DSS, saturable incorporation of radioactivity into 33- or 30-kDa polypeptides was achieved only through using ^{125}I-[α-formyl-Cys_1]apamin (Figure 9). Indeed, even after exhaustive exposure of autoradiograms, no detectable labeling of any polypeptide on membranes from either tissue was observed using ^{125}I-[ϵ-formyl-Lys_4]apamin. Identical results were obtained after repeating these cross-linking experiments using bis[sulfo-succinimido] suberate, which is the water-soluble analogue of DSS (data not shown). Since both ^{125}I-[formyl]apamin derivatives exhibit comparable levels of saturable binding to membranes from either tissue, these results indicate that DSS couples ^{125}I-apamin to its acceptor binding sites solely through the ϵ-amino group of Lys_4.

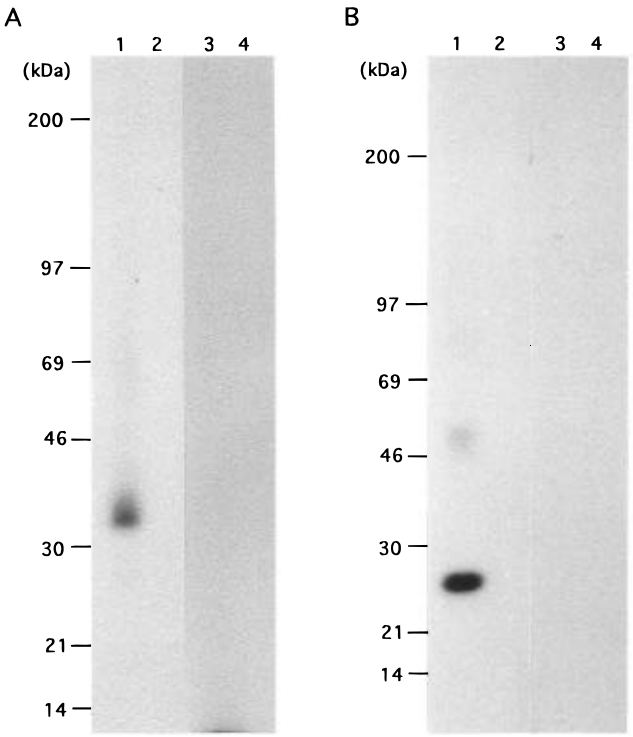

FIGURE 9: Autoradiogram of DSS-mediated cross-linking of ^{125}I-[α-formyl-Cys_1]apamin or ^{125}I-[ϵ-formyl-Lys_4]apamin to brain or liver plasma membranes. Plasma membranes from rat brain (A) or rabbit liver (B) were equilibrated [in 10 mM KCl and 25 mM borax containing 0.1 mM iodoacetamide, 1 mM phenylmethanesulfonyl fluoride, 1 mM EDTA, and 0.1% (w/v) BSA, pH 9.0] with 100 pM of either ^{125}I-[α-formyl-Cys_1]apamin (lanes 1 and 2) or ^{125}I-[ϵ-formyl-Lys_4]apamin (lanes 3 and 4) in the absence (lanes 1 and 3) or presence (lanes 2 and 4) of 0.1 μM native apamin. After washing and resuspension in the presence of 5 mM DSS for 15 min, membranes (~100 μg of protein) were analyzed by gradient pore [4−20% (w/v) acrylamide] SDS−PAGE run under nonreducing conditions.

DISCUSSION

A Rational Strategy for Labeling SK_{Ca} Channel-Associated Polypeptides. Apamin, an octadecapeptide from the venom of the European honeybee *A. mellifera*, is a selective and potent blocker of SK_{Ca} channels and has been used in many biophysical and pharmacological studies to characterize SK_{Ca} channels in diverse tissues and cells (Strong, 1990). Previous biochemical studies using ^{125}I-apamin in cross-linking and photoaffinity labeling strategies have identified high and low molecular mass apamin binding polypeptides thought to be associated with SK_{Ca} channel structure. The patterns of labeling are complex, however, dependent on tissue, the chemical nature of the labeling reagent, and in the case of photolabile derivatives of ^{125}I-apamin even the position of derivatization within the apamin molecule itself. Earlier work of Seagar, Couraud, and colleagues showed that selective coupling of SANPAA to either the α-amino-Cys_1 or ϵ-amino-Lys_4 group of ^{125}I-apamin resulted in labeling on rat brain membranes of two distinct groups of polypeptides of either 86 and 59 kDa, or 33 and 22 kDa, respectively (Seagar *et al*., 1986). Other workers later demonstrated that when ^{125}I-apamin was randomly derivatized with a variety of different photoprobes, only ~30-kDa polypeptides were labeled, with SANPAA uniquely being able to label 86- and 59-kDa species (Auguste *et al*., 1989). In the present study, as part of a systematic approach to the elucidation of SK_{Ca}

Table 1: Labeling of SK_{Ca} Channel-Associated Polypeptides from the α- or ϵ-Amino Position of ^{125}I-Apamin[a]

	high molecular mass polypeptides (86/59 kDa)		low molecular mass polypeptides (~30 kDa)	
photoprobe	α-position	ϵ-position	α-position	ϵ-position
sulfo-HSAB	+	−	−	++
SANPAA	++	−	−	++
sulfo-SAPB	++	−	−	++
sulfo-SANPAH	−	−	++	++

[a] A summary of the general patterns of labeling on rat brain and rabbit liver plasma membranes obtained when various azidoaryl photoprobes are attached to the α-Cys_1 or ϵ-Lys_4 amino groups of either ^{125}I-[ϵ-formyl-Lys_4]apamin or ^{125}I-[α-formyl-Cys_1]apamin. ++, strong labeling; +, weak labeling; −, negligible or no labeling.

channel structure, we have now extended and rationalized these findings. By selectively blocking either the α- or ϵ-amino groups of apamin through formylation, and radioiodinating the resultant monoformyl derivatives, we have been able to unambiguously direct derivatization of ^{125}I-apamin through nucleophilic reaction with the remaining unblocked amino group. We observe that when photoprobes are coupled at the ϵ-amino-Lys_4 position, comparable 33- or 30-kDa polypeptides are efficiently labeled on brain or liver plasma membranes, irrespective of the structure of the photoprobe. However, if ^{125}I-apamin is derivatized at the α-amino-Cys_1 position, labeling becomes critically dependent on the length of the spacer arm in the photoprobe. With the shortest spacer arm very weak labeling of 86- and 59-kDa polypeptides is observed; intermediate spacer arms efficiently label the 86- and 59-kDa polypeptides, whereas a long spacer arm labels the same 33- or 30-kDa polypeptides that are detected from the ϵ-amino position. These findings are summarized in Table 1 and indicate that the spacer arm length, rather than the structure of the photogenerated aromatic nitrene intermediate, is the most important factor governing the selectivity of labeling from the α-amino position of apamin.

In model studies, photolabeling by nitrosubstituted phenyl azides has been reported to be effective only when there is a nucleophilic functional group at the target site because of the short lifetime of the photolytically generated reactive intermediate (Liang & Schuster, 1987). In contrast, unsubstituted phenyl azides give nitrenes which are much longer lived and can, in principle, diffuse away before reacting. However, these differences are unlikely to affect selectivity of labeling in our case, since the photolytically generated intermediates are tethered in the binding site by virtue of being covalently linked to apamin. Nevertheless, structural influences of the reactive intermediate cannot be ruled out completely, since a ~22-kDa polypeptide detected in brain is most effectively labeled from the ϵ-position of apamin when a nitroaromatic nitrene is generated.

Since selective labeling of high or low molecular mass polypeptides can be achieved from the α-Cys_1 position of apamin by photoprobes that differ by only ~5 Å in their extended conformation, this suggests that the 86-, 59-, and 33-kDa polypeptides are very closely associated in the membrane and provides compelling evidence to suggest that SK_{Ca} channels are heterooligomeric. As these structural constraints similarly apply to labeling analogous polypeptides present on either brain or liver plasma membranes, this also suggests a general similarity in the topography of the apamin binding site present on tissue-specific, pharmacologically distinct subtypes of SK_{Ca} channel (see below).

An interesting outcome of the present investigation was the demonstration that considerable differences exist between the reactivity of the α- and ϵ-amino groups of apamin with succinimido ester photoprobes. In accordance with the earlier findings of Seagar *et al*., (1986), derivatization of the ϵ-amino group rather than the α-amino group was much more readily achieved at pH 8.5. At this pH the ϵ-amino group was found to react equivalently with either sulfosuccinimido or succinimido ester photoprobes. In contrast, only by reducing the pH to 6.0 were we able to obtain efficient derivatization of the α-amino group with sulfosuccinimido ester probes, while succinimido ester probes reacted poorly with the α-amino group at either alkaline or acidic pH. These observations are surprising, since at pH 8.5 one would have expected the α-amino group to be fully deprotonated (pK_a 6.7), whereas the ϵ-amino group (pK_a 10.8) should be a relatively poorer nucleophile [pK_a values reported by Okhanov *et al*. (1980)]. Several groups of workers have proposed structures for apamin in solution from NMR studies (Okhanov *et al*., 1980; Pease & Wemmer, 1988; Xu & Nelson, 1994) and this suggests a structural basis for the nucleophilic superiority of the ϵ-amino group. On the basis of these NMR models, the α-amino group appears to reside in a pocket created by the Cys_1-Cys_{11} disulfide bridge and the α-helical backbone of the toxin, where it is believed to form a salt bridge with the carboxyl side chain of Glu_7. In comparison, the ϵ-amino group is exposed on the surface of the toxin and is readily accessible. The reduced nucleophilicity of the α-amino group as well as differences in the reactivity of the α-amino group, with polar sulfosuccinimido versus nonpolar succinimido ester probes, may be attributable to steric factors governing accessibility to the pocket enclosing the salt bridge. In agreement with the earlier deductions of Seagar *et al*. (1986), we have now shown that the readily accessible ϵ-amino group of Lys_4 is the sole position involved in DSS-mediated cross-linking of ^{125}I-apamin to its acceptor binding sites. Since we have now conclusively demonstrated that high molecular mass (86 and 59 kDa) polypeptides cannot be labeled from the ϵ-amino position, these findings explain why coupling of ^{125}I-apamin with DSS always results in labeling of low molecular mass (~30-kDa) polypeptides (Hugues *et al*., 1982b; Schmid-Antomarchi *et al*., 1984; Auguste *et al*., 1989; Wadsworth *et al*., 1994).

SK_{Ca} Channel Subtypes Display Conserved Organization of Their Polypeptide Subunits. We have previously provided evidence for the existence of distinct SK_{Ca} channel subtypes in brain or liver that are distinguished by the presence of either 33- or 25−30-kDa apamin binding polypeptides (Wadsworth *et al*., 1994). Such structural variations may underlie recently discovered differences in the pharmacology of neuronal and hepatic SK_{Ca} channels (Dunn *et al*., 1996). Our ability to rationally label high (86- and 59-kDa) and low (33- or 30-kDa) molecular mass apamin binding polypeptides on brain and liver plasma membranes has revealed underlying structural features that appear to be generally conserved among SK_{Ca} channel subtypes. Specifically, all SK_{Ca} channels appear to comprise heterooligomeric complexes containing high and low molecular mass polypeptide subunits. In agreement with the previously documented conservation of the neuronal 33-kDa apamin binding polypeptide between species (rat, guinea pig, bovine, and rabbit

brains) (Wadsworth *et al*., 1994), we now show similar conservation of the 86- and 59-kDa polypeptides (rat, guinea pig, and rabbit brains). Clearly, these data point to a conserved structure(s) for neuronal SK_{Ca} channels in mammalian brain. In mammalian liver, on the other hand, the situation is still somewhat complex. Previously identified distinct ~25−30-kDa polypeptide counterparts of the neuronal 33-kDa polypeptide (Wadsworth *et al*., 1994) appear to be coexpressed with both the 86- and 59-kDa polypeptides (guinea pig liver) or the 59-kDa polypeptide alone (rabbit liver). However, the observation that the 86-kDa polypeptide can be detected in the absence of the 59-kDa species on cultured neurons from rat brain (Seagar *et al*., 1986), cultured cells from rat heart (Marqueze *et al*., 1987), and smooth muscle membranes from guinea pig ileum (Marqueze *et al*., 1987) indicates that coexpression of both the 86- and 59-kDa polypeptides may not be a prerequisite for the expression of functional SK_{Ca} channels. These findings return us to questioning the origins of the 59-kDa polypeptide and whether it represents a degradation product or a specifically truncated isoform of the 86-kDa polypeptide (Leveque *et al*., 1990). From our present results we have no evidence for the 59-kDa species being a nonspecific degradation product. All brain and liver tissue is rapidly processed at low temperature in the presence of a cocktail of protease inhibitors, which is maintained during all subsequent experimental manipulations. The relative labeling intensities of the 86- and 59-kDa polypeptides are consistent between the brains of all species that we have examined and between several different preparations of membranes within each species. At no time have we seen any evidence of proteolytic nicking as evidenced by laddering of labeled bands. If the 59-kDa polypeptide is a product of the same gene as the 86-kDa polypeptide, then it is most probably as a result of alternative splicing or specific posttranslational proteolytic processing. Since the 59-kDa polypeptide is observed in the apparent absence of the 86-kDa polypeptide in rabbit liver (and nonspecific proteolysis is ruled out for the same reasons discussed above), we would like to speculate that the 59-kDa polypeptide may function as an alternative subunit of the larger molecule. If this is true, and 86- and 59-kDa polypeptides are tentatively assigned as alternative α-subunits and the ~30-kDa polypeptides as alternative β subunits, then heterooligomeric SK_{Ca} channel subtypes containing different α- and β-subunits may reflect fine-tuning of SK_{Ca} channel function to suit particular physiological roles. This situation has been demonstrated for other classes of ion channels, and in the case of heterooligomeric α-dendrotoxin-sensitive voltage-dependent K^+ channels from bovine cortex (Parcej *et al*., 1992), it is known that at least half of these channels contain more than one subtype of α-subunit (Scott *et al*., 1994). Although our understanding of SK_{Ca} channel structure is far less advanced and the relative stoichiometry of putative α- and β-subunits within functional SK_{Ca} channel complexes has yet to be established, one can speculate that the total copy number of α- and β-subunits may be conserved among SK_{Ca} channel subtypes. Structural diversity may thus originate from variation in the content of individual α- and β-subunits, as evidenced by the demonstrable tissue- and cell-specific variation in expression of particular apamin binding polypeptides. The ability to now rationally and selectively label high and low molecular mass polypeptides associated with apamin-sensitive SK_{Ca} channel subtypes is an important step toward determining the validity of these hypotheses.

ACKNOWLEDGMENT

We thank Dr. J. C. Fernandez-Masaguer (on leave from the University of Santiago de Compostela) for the synthesis of SANPAA and Dr P. B. Bishop (University College, London) for helpful discussion on the chemistry of photoaffinity labels. We are grateful to Dr. P. Bolwell (Royal Holloway College, London) for performing amino acid sequencing and to Dr. B. S. Brewster for helpful discussions. Our thanks are also due to Mrs. K. Davidson for photography.

REFERENCES

Auguste, P., Hugues, M., & Lazdunski, M. (1989) *FEBS Lett. 248*, 150−154.
Bernatowicz, M. S., & Matsueda, G. R. (1986) *Anal. Biochem. 155*, 95−102.
Brewster, B. S., & Strong, P. N. (1992) in *Potassium Channel Modulators* (Weston, A. H., & Hamilton, T. C., Eds.) pp 272−303, Blackwell Scientific Publications, Oxford, England.
Dempsey, C. E. (1982) *J. Chem. Soc., Perkin Trans. 1*, 2625−2629.
Dunn, P. M., Benton, D. C. H., Campos Rosa, J., Ganellin, C. R., & Jenkinson, D. H. (1996) *Br. J. Pharmacol. 117*, 35−42.
Habermann, E., & Fischer, K. (1979) *Eur. J. Biochem. 94*, 355−364.
Hugues, M., Duval, D., Kitabgi, P., Lazdunski, M., & Vincent, J.-P. (1982a) *J. Biol. Chem. 257*, 2762−2769.
Hugues, M., Schmid, H., & Lazdunski, M. (1982b) *Biochem. Biophys. Res. Commun. 107*, 1577−1582 .
Laemmli, U. K. (1970) *Nature 227*, 680−685.
Leveque, C., Marqueze, B., Couraud, F., & Seagar, M. (1990) *FEBS Lett. 275*, 185−189.
Liang, T.-Y., & Schuster, G. B. (1987) *J. Am. Chem. Soc. 109*, 7803−7810.
Marqueze, B., Seagar, M. J., & Couraud, F. (1987) *Eur. J. Biochem. 169*, 295−298.
Ofengand, J., Schwartz, I., Chinali, G., Hixson, S. S., & Hixson, S. H. (1977) *Methods Enzymol. 46*, 683−702 .
Okhanov, V. V., Afanasev, V. A., Gurevich, A. Z., Elyakova, E. G., Miroshnikov, A. I., Bystrov, V. F., & Ovchinnikov, Yu. A. (1980) *Sov. J. Bioorg. Chem. (Engl. Transl.) 6*, 840−864.
Parcej, D. N., Scott, V. E. S., & Dolly, J. O. (1992) *Biochemistry 31*, 11084−11088.
Pease, J. H. B., & Wemmer, D. E. (1988) *Biochemistry 27*, 8491−8498.
Schmid-Antomarchi, H., Hugues, M., Norman, R., Ellory, C., Borsotto, M., & Lazdunski, M. (1984) *Eur. J. Biochem. 142*, 1−6.
Scott, V. E. S., Muniz, Z. M., Sewing, S., Lichtinghagen, R., Parcej, D. N., Pongs, O., & Dolly, J. O. (1994) *Biochemistry 33*, 1617−1623.
Seagar, M. J., Labbé-Jullié, C., Granier, C., Van Rietschoten, J., & Couraud, F. (1985) *J. Biol. Chem. 260*, 3895−3898.
Seagar, M. J., Labbé-Jullié, C., Granier, C., Goll, A., Glossmann, H., Van Rietschoten, J., & Couraud, F. (1986) *Biochemistry 25*, 4051−4057.
Strong, P. N. (1990) *Pharmacol. Ther. 46*, 137−162.
Strong, P. N., & Brewster, B. S. (1992) *Methods Neurosci. 8*, 15−24.
Takanashi, H., Sawanobori, T., Kamisaka, K., Maezawa, H., & Hiraoka, M. (1992) *Jpn. J. Physiol. 42*, 415−430.
Vincent, J. P., Schweitz, H., & Lazdunski, M. (1975) *Biochemistry 14*, 2521−2525.
Wadsworth, J. D. F., Doorty, K. B., & Strong, P. N. (1994) *J. Biol. Chem. 269*, 18053−18061.
Xu, X., & Nelson, J. W. (1994) *Biochemistry 33*, 5253−5261.

BI9602371